网络优先出版,实际出版页码及内容以正式版为准

第55卷第8期 2026年8月 光子学报 ACTA PHOTONICA SINICA Vol.55 No.8 August 2026

引用格式: DENG Xue, XUE Wenxiang, HE Zaimin, et al. Investigation of Phase Noise Compensation Methods for Optical Frequency Transfer[J]. Acta Photonica Sinica, 2026, 55(8):0806002

邓雪,薛文祥,何在民,等. 光学频率传递相噪补偿方法研究[J]. 光子学报,2026,55(8):0806002

光学频率传递相噪补偿方法研究

邓雪[1,2,3],薛文祥[1,2,3],何在民[1,2,3],广伟[1,2,3],张翔[4],焦东东[4]

(1 西安邮电大学 通信与信息工程学院,西安 710121)

(2 陕西省信息通信网络及安全重点实验室,西安 710121)

(3 陕西高校青年创新团队,西安 710121)

(4 中国科学院国家授时中心,西安 710600)

摘　要:提出一种增强型相噪补偿方法,将实时相噪消除技术与后处理算法相结合,在时间上对齐补偿信号与噪声信号后再进行二次抵消,能够降低路径时延影响,进而提升系统噪声抑制能力。仿真与实验验证,所提方法传递精度较传统被动补偿方案提升了4倍,可用于支持远程原子钟比对等光频传递应用场景。

关键词:光纤链路及系统;相位噪声抑制;频率传递;光纤;自由空间

中图分类号:O439　　**文献标识码**:A　　**doi**:10.3788/gzxb20265508.0806002

0　引言

近年来,光纤光学频率传递技术已展现出传输精度高、距离远、鲁棒性强等优越性能[1-3]。目前,基于光纤的光频传递系统已在数千公里长度范围内实现日稳定度10^{-21}量级的传递精度,为高精度光频比对[4]、暗物质探测[5]和甚长基线干涉测量[6]等前沿科学应用提供了重要技术支撑。另一方面,自由空间光频传递也在百公里距离上取得了10^{-19}量级的稳定度[7-8],为山区、星际等无法铺设光纤的场景提供了可行的传递方案。

为了确保信号的高保真传递,现有系统通常将部分传输信号反射回本地进行相位检测与实时补偿[9-11],从而有效抑制由光纤或自由空间链路中路径长度变化与折射率起伏所引起的多普勒噪声。然而,当链路本征噪声被抑制至理论极限后,残留相位噪声成为限制传递精度(尤其是短期稳定度)的主要因素,这一问题在长距离传输中尤为突出。例如,长度为100公里的光纤链路在1秒平均时间下的稳定度通常介于10^{-15}至10^{-16}之间[12-13],而500公里链路的稳定度则进一步下降至约10^{-14}量级[11,14],这一数值显著差于目前最先进的超稳激光器[15-16]或光学原子钟[17-18]所能提供的10^{-17}量级短期精度。因此,进一步提升光频传递系统的精度,仍是当前研究的重要技术目标。

在传统相位噪声抑制方案中,光信号在链路中的传输延迟会导致反馈补偿的时间滞后,进而限制相位控制带宽。研究表明,相位噪声消除理论极限与光传输时延及噪声频率呈反比关系[19-20]。采用级联传输架构可有效提升相噪补偿能力,该架构将长距离链路划分为多个较短区段,并在每一段独立进行相位噪声补偿,从而提高了系统的整体补偿带宽[21]。2021年,法国研究团队报道了一种基于级联结构的分布式光频传递网络,通过十余个中继站构建了总长度达4800km的传递网络[1],实现了多节点光频传递,在2000秒平均时间下的稳定度达到1×10^{-19}。其中,中继站的核心功能包括光学放大与单段线路的相位噪声消除。尽管级联方案能够有效拓展传递距离并支持网络分支扩展,但也显著增加了系统的复杂性与成本。

基金项目:国家自然科学基金(12403078,12303077),西安市科协青年人才托举计划(0959202513075),陕西省重点研发计划(2024GX－ZDCYL－01－28,2025CY－YBXM－0060),三秦特殊支持计划(09R0557A00),陕西省杰出青年科学基金项目(2025JC－JC-QN－082),陕西省秦创原"科学家＋工程师"团队建设项目(2025QCY－KXJ－162)

第一作者:邓雪,dengxue@xupt.edu.cn

通讯作者:张翔,zhangxiang@ntsc.ac.cn;焦东东,jiaodd@ntsc.ac.cn

收稿日期:2026－04－01;**录用日期**:2026－07－01

鉴于反馈滞后是相噪无法被完全补偿的主要原因，本文提出一种融合实时消除与后处理校正的增强型相位噪声抑制方法，该双补偿策略在完成实时噪声抑制的基础上，通过二次后处理减小传输信号与补偿信号间的时序失配，从而提升系统整体性能，为长距离光频传递应用提供技术支撑。

1　相噪补偿方案原理

如图1所示，光频传递链路中，通过迈克尔逊干涉仪结构消除相位噪声。传递链路充当信号臂，末端连接法拉第镜2(FM2)，一段短光纤作为参考臂，末端连接法拉第镜1(FM1)。法拉第镜用于反射激光信号并稳定信号的偏振，确保光电探测器能够检测到功率稳定的拍频干涉信号。拍频信号携带双程光纤噪声，对拍频信号进行处理再反馈至声光调制器1(AOM1)即可实时补偿相噪。根据是否采用锁相环，光频传递噪声消除方案可分为主动式与被动式两类[11,22]，图1中的(a)、(b)分别展示了主动方案和被动方案的系统原理。在主动补偿方案中，锁相环用于解调相位误差，并将其反馈至声光调制器的射频驱动器来补偿噪声。而被动方案则无需锁相环，直接将拍频信号频率做二倍分频并驱动声光调制器实现噪声补偿。这两种方案均可采用本文所提出的噪声增强补偿方法，以进一步提升传递精度。

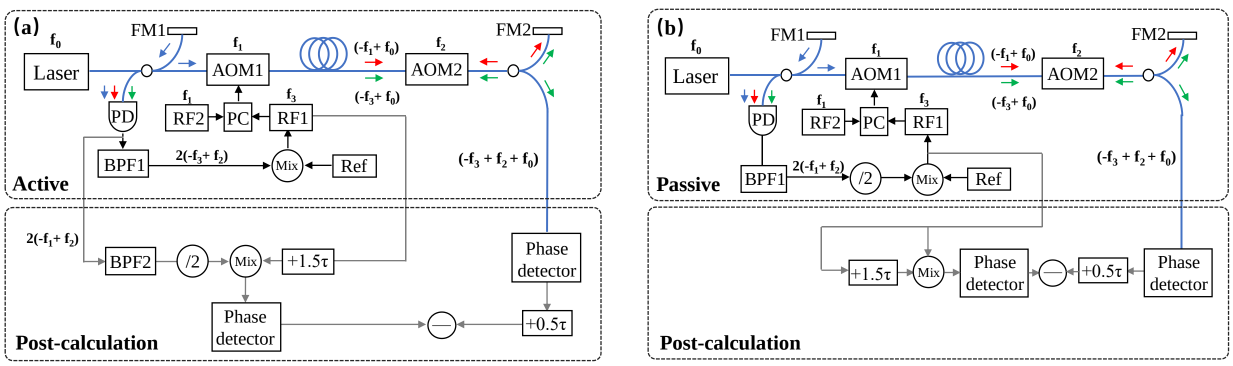

图1　噪声增强补偿方法原理图。(a)主动相位噪声补偿方案原理图；(b)被动相位噪声补偿方案原理

Fig. 1　Enhanced noise compensation schematic diagram. (a) Optical frequency transfer link with active phase noise cancellation; (b) Optical frequency transfer link with passive phase noise cancellation

PD: Photo Diode; BPF: Band－Pass Filter; RF: Radio Frequency Source; MIX: Mixer; FM: Faraday Mirror; AOM: Acousto－Optic Modulator; PC: Power Coupler

对所提方案进行理论推导。在$(t+\tau)$时刻，传输信号单次通过传输介质(如光纤和自由空间)后所累加的相位抖动可表示为[19]

$$\varphi_{\text{single}}(t+\tau)=\int_0^L \delta\varphi(z,\ t+z/c_n)\mathrm{d}z \tag{1}$$

式中，τ为传递时延，在t时刻，通过本地拍频信号探测的双程光纤相位抖动可表示为

$$\varphi_{\text{double}}(t)=\int_0^L\left[\delta\varphi(z,\ t-z/c_n)+\delta\varphi(z,\ t-(2\tau-z/c_n))\right]\mathrm{d}z \tag{2}$$

在$(t+\tau)$时刻，经补偿后传递信号残余相位噪声$\varphi_{\text{residual}}(t+\tau)$表示为

$$\varphi_{\text{residual}}(t+\tau)=\varphi_{\text{single}}(t+\tau)-\varphi_{\text{compe}}(t) \tag{3}$$

式中，$\varphi_{\text{compe}}(t)$为补偿信号，对于被动补偿方案来说，$\varphi_{\text{compe}}(t)=1/2\cdot\varphi_{\text{double}}(t)$，对于主动方案，$\varphi_{\text{compe}}(t)$与锁相环参数相关。通过式(1)(2)(3)可以看出，补偿信号的时序滞后于传递信号，从而限制了补偿带宽。这里，我们引入一个校正量$\varphi_{\text{post}}(t)$来重新对齐传递信号和补偿信号的时序

$$\varphi_{\text{post}}(t)=1/2\cdot\varphi_{\text{double}}(t+\delta\tau)-\varphi_{\text{compe}}(t) \tag{4}$$

然后，通过后期处理的方式将校正信号反馈给传递信号，实现增强补偿

$$\varphi_{\text{enhanced}}(t+\tau)=\varphi_{\text{residual}}(t+\tau)-\varphi_{\text{post}}(t) \tag{5}$$

$\varphi_{\text{enhanced}}$代表经校正后的传递信号相噪，对式(5)进一步计算，可得

$$\varphi_{\text{enhanced}}(t+\tau)=\varphi_{\text{single}}(t+\tau)-1/2\cdot\varphi_{\text{double}}(t+\delta\tau)\approx\int_0^L(\tau-\delta\tau+z/c_n)\cdot\frac{\mathrm{d}\delta\varphi}{\mathrm{d}t}\mathrm{d}z \tag{6}$$

对式(6)进行傅里叶变换并计算功率谱密度,可得

$$S_{\text{enhanced}}(\omega)\approx\int_0^L\left(\tau-\delta\tau+\frac{z}{c_n}\right)^2\cdot\omega^2\cdot\delta S(\omega)\mathrm{d}z=\frac{\omega^2}{L}\cdot S_{\text{single}}(\omega)\cdot\int_0^L\left(\tau-\delta\tau+\frac{z}{c_n}\right)^2\mathrm{d}z \tag{7}$$

进一步化简,得

$$S_{\text{enhanced}}(\omega)=\frac{\omega^2}{3\tau}\cdot S_{\text{single}}(\omega)\cdot\left[(2\tau-\delta\tau)^3-(\tau-\delta\tau)^3\right] \tag{8}$$

根据式(8)可以推导出,当 $\delta\tau=\frac{3}{2}\tau$ 时,S_{enhanced} 具有最小值:$\frac{1}{12}(\omega\tau)^2\cdot S(\omega)$。相较于传统主动抑制方法[20]与被动抑制方法[23]的理论极限 $\frac{1}{3}(\omega\tau)^2\cdot S_{\text{single}}(\omega)$ 与 $\frac{7}{3}(\omega\tau)^2\cdot S_{\text{single}}(\omega)$,所提方法的噪声抑制能力是主动方案的4倍,被动方案的28倍。

为实现增强型相位噪声抑制,需对自由运转拍频信号及实时补偿信号进行附加测量。如图1所示,可利用功率耦合器将两个频率有微小不同的射频信号反馈给声光调制器,其中一路信号用于链路噪声检测,另一路信号用于实时相位噪声补偿。校正信号可以通过混频器生成。根据前文推导结果,给予补偿信号 $\frac{3}{2}\tau$ 延迟并与自由运转信号混频鉴相,即可获得校正信号,在用户端将传输信号在时序上延迟 $\frac{1}{2}\tau$,与校正信号作差分处理,即可实现相噪抑制增强。对于被动补偿方案,自由运转信号也是补偿信号,将其分为两路,进行延迟差分即可。信号时序上的延迟可通过数字电路实现。

2 仿真实验及结果分析

为验证所提方法的有效性,开展了300公里光纤光频传递仿真。仿真中,将光纤划分为30个区段,模拟了激光在光纤传输中的相位噪声累积过程,对主动与被动两种补偿方案的噪声抑制机制进行了仿真,并评估了本文所提方案相位噪声抑制效果。基于实际光纤链路的功率谱密度特性构建了相位噪声模型[10-11,19-20],如式(9)所示,其中单区段的 h 值设为 $500\mathrm{rad}^2/\mathrm{Hz}$。

$$S_{\text{single}}(f)=\begin{cases}\dfrac{h}{f^2},\ f<1\mathrm{kHz}\\[2ex]\dfrac{h}{1000\cdot f^3},\ f\geqslant 1\mathrm{kHz}\end{cases} \tag{9}$$

依据式(9)所示的相噪模型获得了对应的时域相位抖动信号,如图2(a)所示,显示了00公里光纤所引入的单程(环外信号)与双程(环内信号)相位抖动,以及通过锁相环进行噪声抑制后的残余相位抖动。可以看到,单程与双程相位抖动具有显著相关性,且单程相位抖动经过锁相后得到大幅抑制。仿真实验中,相位噪声抑制的仿真遵循实际物理过程,由于环内激光信号两次通过AOM,因此,环内相位的锁定是瞬时反馈和延时反馈的叠加。在实际系统中,除传递光纤以外,光纤链路中的各类器件均会引入噪声,包括光学放大器、连接光纤、探测器及信号参考源等。链路中通常采用单纤双向掺铒光纤放大器(Bi-EDFA)或布里渊放大器(FBA)进行光放大[4,10-11,14]。由于放大器的增益光纤已接入传递光纤,或放大器本身即以传递光纤作为增益介质[24],因此放大器引入的相位抖动可与传递光纤自身的相位抖动一并得到补偿。此外,放大过程中产生的宽带噪声可通过光学滤波器或光学锁相环加以抑制[25-26]。所以,在满足一定信噪比条件(通常为30dB以上)时,放大器噪声对系统鉴相及噪声补偿的影响可忽略不计[25]。探测器引入的噪声,与传递系统中连接光纤受环境扰动产生的噪声,以及鉴相器、信号参考源等其他电路噪声,共同构成系统的本底噪声。通过缩短连接光纤长度、对光路进行温控、采用高稳原子钟作为参考或对连接光纤噪声进行主动控制等措施[12,27],可有效降低系统本底噪声,使其达到秒稳 10^{-18}、万秒稳 10^{-21} 甚至 10^{-22} 量级[3,27]。可知,当补偿后的传递噪声大于系统本底噪声时,本底噪声不会影响传递精度[11-13,22-23]。因此,本文在仿真中假设其他器件引入的噪声已得到有效控制,重点考虑光纤线路的相位噪声的抑制效果。仿真参数为:采样率20 kHz(对应距离

分辨率为10km），采样点数10^7。为了便于显示，图2数据进行了因子为20的平均处理。

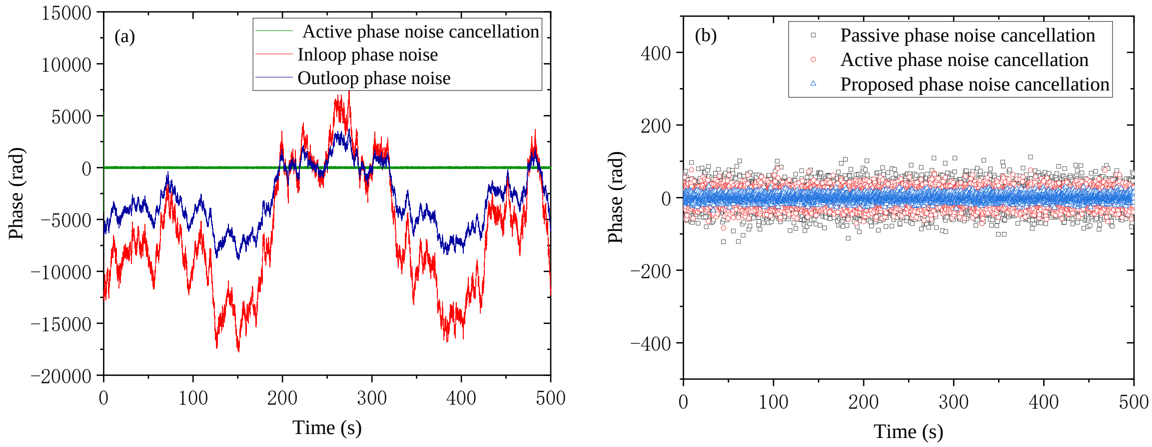

图2　传递信号相位噪声。(a)300km光纤引入的相位抖动，分别为自由运转环外、环内相位抖动和锁定环外相位抖动；(b)主动方案、被动方案和增强方案对应的补偿后的相位抖动

Fig. 2　Phase noise of transferred signal. (a) Phase jitter of the 300 km fiber under free-running out-loop, in-loop, and stabilized single-trip conditions; (b) Phase jitter of active stabilization, passive stabilization and the enhanced stabilization

图2(b)对比了传统主动相位噪声抑制方法、被动相位噪声抑制方法与本文所提增强型相位抑制方法对应的相位抖动。可以看到，被动方法对应的残余相位抖动最大，主动方法次之，而所提方法则成功将噪声抑制至更低水平。图3给出了对应的相位噪声功率谱密度，为便于对比，同时给出了根据式(9)计算的理论功率谱密度曲线。结果显示，在带宽内，仿真相位噪声与理论值较为一致，验证了仿真的准确性。其中，主动方法在低频段相位噪声略高于理论值，这是为了兼顾锁相环在低频与高频段的锁定效果，对环路滤波器参数进行了折衷。由图3可知，自由运行链路在1 Hz处的功率谱密度为2.0×10^4 rad^2/Hz，被动方法为3.1 rad^2/Hz，主动方法为0.7 rad^2/Hz，增强型方法为0.1 rad^2/Hz。在144 Hz处，主动方法相位噪声出现了一个尖峰，该现象源于锁相环在环路锁定带宽处的振荡。

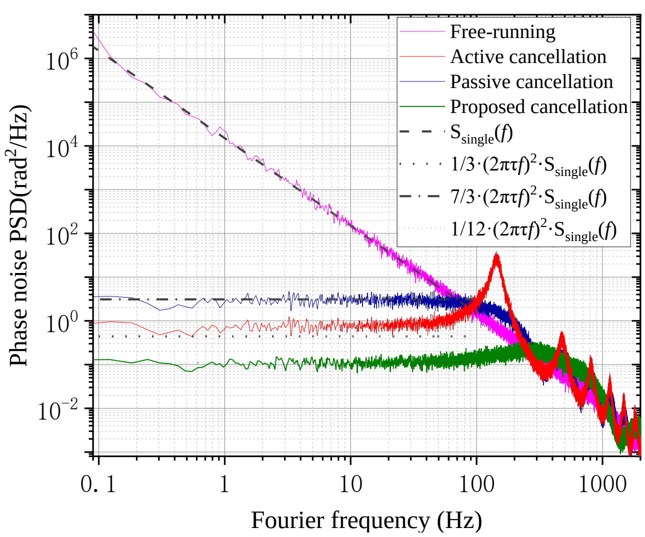

图3　传统主动方案、被动方案和增强方案对应的相位噪声功率谱密度

Fig. 3　Phase noise power spectral density of active stabilization, passive stabilization and the enhanced stabilization

本文对三种相噪抑制方法对应的传递稳定度进行了计算，如图4所示。自由运转链路在1秒平均时间下的MDEV为2.8×10^{-13}，被动稳定方法对应的MDEV为1.6×10^{-15}，主动稳定方法为8.0×10^{-16}，增强型稳定方法为3.3×10^{-16}。在100秒平均时间下，增强型稳定方法的MDEV达到4.6×10^{-19}。可以看出，对于传递稳

定度,增强型方法较主动方法改善约1倍,较被动方法改善约4倍,这也与$\sigma \sim \sqrt{S(\omega)}$的理论关系一致。

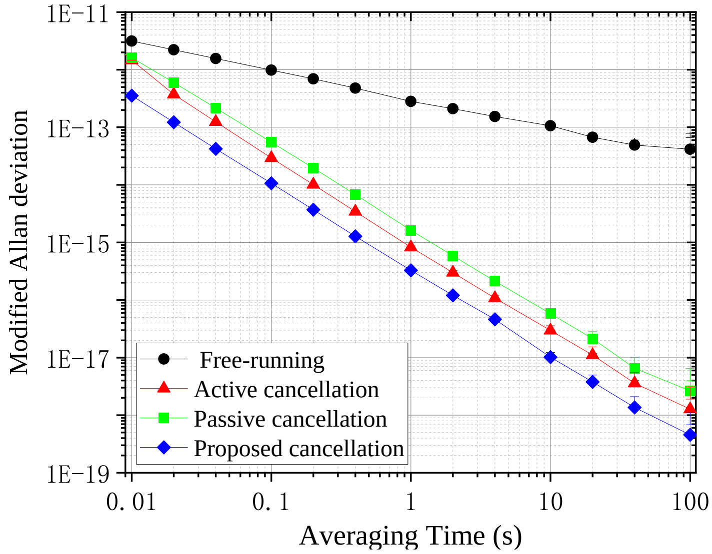

图4 自由运行链路(圆形实线)、主动稳定方法(三角形实线)、被动稳定方法(方形实线)及增强型稳定方法(菱形实线)的修正阿伦偏差。

Fig. 4 Modified Allan deviation of free-running link (circles), active stabilization link (triangles), passive stabilization link (squares) and the enhanced stabilization link (diamonds)

值得注意的是,为实现增强型相位噪声补偿,需要保持传递两端频率计数设备的时间同步(因测量设备位于传递线路两端,其各自独立测量无法确保启动时间一致),以完成后续计算所需的时间对齐。因此,本文分析了时间同步偏差对相位噪声抑制效果的影响。计算了在不同$\delta\tau$取值情况下,增强型稳定方法与传统方法在1 Hz至10 Hz频段内功率谱密度平均比值的变化情况。结果显示,当$\delta\tau=1.5\tau$时,增强效果达到最优;若$\delta\tau$偏离最优值$\pm 0.5\tau$,增强效果将降至原来的1/4;当$\delta\tau$偏离$\pm 0.1\tau$,增强效果仍可保持最优值的90%。因此,在实际应用中需将时间同步误差控制在0.1τ以内,对于300公里光纤链路,0.1τ约为0.15毫秒,实现该量级的时间同步在技术上较为可行,例如在同一光纤线路中,可通过波分复用技术实现光学频率信号、时间信号及微波信号的同时传递,从而同时满足频率传递与时间同步的需求[28]。时间同步可以通过回环法和双向比对法对链路的时延进行测量[29-30],并通过数字电路延迟线或FPGA实现时延控制,同步精度优于百纳秒,当结合精密锁相的时差补偿技术时,甚至可实现皮秒量级的时间同步精度[30]。

3 实地光纤链路测试

在490km实地光纤链路上对所提增强型相位噪声补偿方案进行了测试,重点对比了传统被动相噪抑制方法和所提方法的传递精度。该光纤链路为西安到汉中的通信光纤链路,长度245km,将两段同样长度的光纤在汉中相连构成了总长度为490km的链路。为了补偿光纤损耗,系统中使用了7个掺铒光纤放大器(EDFA)进行光学放大。通过同一个频率计数器同时测试实时锁定传递信号和本地自由运转环内信号,并按照所提方法在后期调整其相对时延并作差实现相噪抑制增强。这里利用频率计数器的测量时间间隔调整相对时延,时间间隔为1ms,对于490km长度来说,1ms即对应0.41τ,加上传递链路固有时延τ,因此可设置的离目标值最接近的时延值为1.41τ,频率作差后计算其稳定度,结果如图5所示。

可以看到,所提增强抑制方案的精度相较于传统被动锁定方法有着明显的提升,在1s处的ADEV改善了约4.37倍,略优于理论值,验证了本方案的有效性。在较短平均时间内(0.01s~1s),增强方案的改善效果略优于理论值,我们分析原因可能是490km光纤相噪抑制带宽位于100Hz附近,而增强方案能够有效提升控制带宽,因此对该频段噪声有一定的抑制效果,从而提升了传递短时稳定度。此外,以0.41τ为间隔设置了不同时延,观察到随着时延增加,抑制效果呈现先增强后减弱的趋势,这与式(8)反映的规律一致。

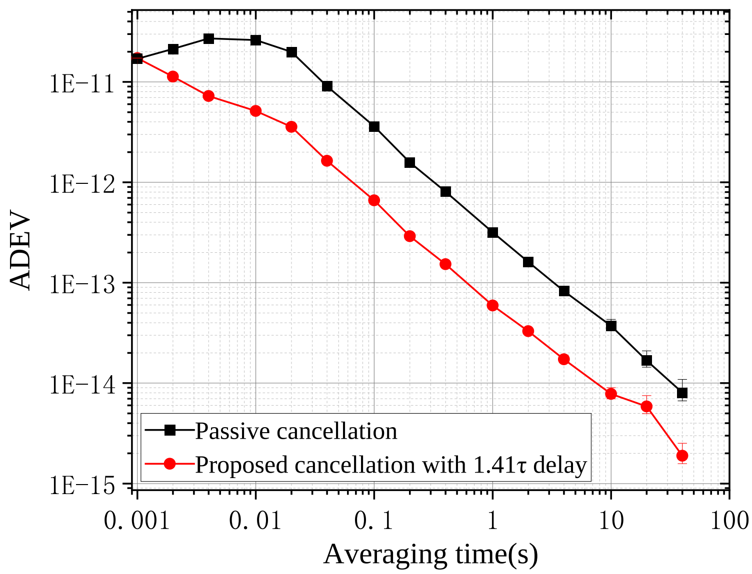

图5 传统被动锁定方法(方形实线)及增强型稳定方法(圆形实线)的阿伦偏差

Fig. 5 Allan deviation of traditional passive cancellation (squares) and the enhanced stabilization link (circles)

4 周跳的抑制研究

周跳是导致传输信号质量下降的另一个重要因素,其产生与多个因素相关,包括器件的相位检测范围、外部环境干扰以及信噪比恶化等。实验表明,当鉴相动态范围不足时,传递线路相位将无法准确探测及补偿,进而引发锁相环相位跳变,最终影响传递信号精度[23]。通过增大鉴相系统分频倍数或采用相位延展技术,可有效提升鉴相动态范围[23,31],从而降低周跳发生的频次。本文重点研究主动相位抑制方案中由鉴相器动态范围有限而引发的周跳问题,并验证了本文所提方法消除周跳的有效性。具体方案如下,为了模拟鉴相器的有限的动态范围,在获得的相位误差信号中设置了±70弧度的相位测量范围,该范围通过在误差信号上引入卷绕算法实现,以模拟实际鉴相系统中相位周期性折叠的特性[11,31]。结果如图6所示,当相位噪声超出该范围时,周跳随之产生,传递精度随之恶化。作为对比,图6同时展示了采用增强方案后的结果。本文所提增强方案利用频率计数器对传递信号的补偿信号与自由运转信号进行充分的相位检测。由于频率计数器的测量范围(通常为几十兆赫兹至上百兆赫兹)远大于传递信号的频率抖动范围,增强方案能够准确测量自由运转环内信号以及发生周跳的补偿信号,并在后期处理环节中有效消除,结果如图6所示。上述研究仅考虑了鉴相动态范围对周跳现象的影响,而实际系统中信噪比恶化也是诱发周跳的重要原因[32-33],尤其长距离传输线路,随着光学放大器的使用,信噪比恶化难以避免。因此需精密设置放大器参数(如增益、间隔距离等),以尽可能抑制信噪比的恶化[34]。此外,在级联传递方案中,采用光学再生放大技术将本地激光相位锁定至传递信号,亦可有效提升激光信噪比。尤其当选用低噪声超稳激光作为本地激光时,其效果将更为显著[35]。结合本文所提增强方案,有望将周跳率降到10^{-5}以下。

5 结论

综上所述,本文提出了一种用于光频传递链路的增强型相位噪声补偿方法。该方法通过在本地端对传递信号进行实时补偿,并测量相噪补偿校正信号,再通过后处理将校正信号从传输信号中消除,从而提高传链路性能。通过对光纤相位噪声的累积与补偿过程进行仿真,验证了理论推导的准确性。结果显示,所提方法的噪声抑制效果是传统主动方案的4倍。通过在490km实地光纤链路上进行测试,进一步验证了所提方案的有效性。此外,本文还分析了链路两端设备时间同步偏差对方案性能的影响,并对周跳现象的抑制效果进行了仿真验证。本方法的相位增强基于后处理实现,因此在光频比对等具备后处理环节的应用中具有较好的适用性。然而,对于依赖实时处理的相关应用,增强方案受限于“后补偿”性质,在后期处理环节中引入最少1.5τ的时延,对于百公里级光纤,时延约为毫秒量级。后续可通过优化实验方案来增强实时性,例

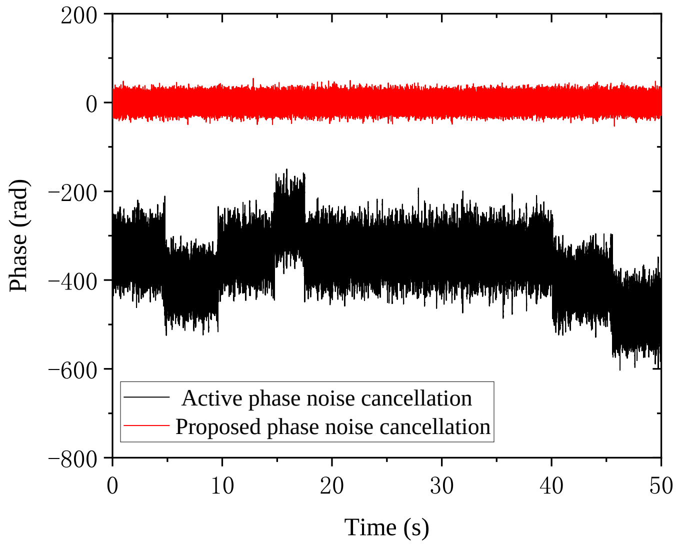

图6　传统主动方案周跳仿真及增强方案对周跳的消除效果

Fig. 6　Transferred phase of active phase stabilization with cycle slips and proposed phase stabilization without cycle slips

如通过高精细度光学参考腔在光学路径上对传递信号进行延迟处理,从而实现补偿信号与传递信号的时间对齐。

参考文献

[1] CANTIN E, TØNNES M, TARGAT R L, et al. An accurate and robust metrological network for coherent optical frequency dissemination[J]. New Journal of Physics, 2021, 23(5): 053027.

[2] KOKE S, KUHL A, WATERHOLTER T, et al. Combining fiber Brillouin amplification with a repeater laser station for fiber-based optical frequency dissemination over 1400 km[J]. New Journal of Physics, 2019, 21(12): 123017.

[3] KADUM E J, JI Jingxian, KUHL A, et al. Optical frequency transfer with below 10^{-21} uncertainty using a DFB - laser-based fiber Brillouin amplifier[J]. APL Photonics, 2023, 8(3): 036113.

[4] LISDAT C, GROSCHE G, QUINTIN N, et al. A clock network for geodesy and fundamental science[J]. Nature Communication, 2016, 7(1): 12443.

[5] FILZINGER M, CADDELL R A, JANI D, et al. Ultralight dark matter search with space-time separated atomic clocks and cavities[J]. Physical Review Letters, 2025, 134(3): 031001.

[6] CLIVATI C, AIELLO R, BIANCO G, et al. Common-clock very long baseline interferometry using a coherent optical fiber link[J]. Optica, 2020, 7(8): 1031-1037.

[7] SHEN Qi, GUAN Jianyu, REN Jigang, et al. Free-space dissemination of time and frequency with 10^{-19} instability over 113 km[J]. Nature, 2022, 610(7933): 661 - 666.

[8] YANG J, KANG J H, LEE K, et al. Phase-stabilized free-space link for optical frequency transfe[J]r. Optics Communications, 2022, 504: 127481.

[9] HU Zhenyuan, YUE Yaoli, ZHANG Yanyan, et al. Noise suppression of frequency transfer on short-distance optical fiber link based on 3×3 fiber coupler[J]. Acta Photonica Sinica, 2023, 52(1): 0106002.
胡珍源,岳耀笠,张颜艳,等.一种基于3×3光纤耦合器的短距离光纤频率传递的噪声抑制方法[J].光子学报,2023,52(1):0106002.

[10] RAUPACH S M F, KOCZWARA A, GROSCH E. Optical frequency transfer via a 660 km underground fiber link using a remote Brillouin amplifier[J]. Optics Express, 2014, 22(22): 26537.

[11] ZHANG Xiang, DENG Xue, ZANG Qi, et al. Coherent optical frequency transfer via a 490 km noisy fiber link[J]. Chinese Physics Letters, 2022, 39(4): 044201.

[12] ZHANG Xiang, ZHOU Qian, ZANG Qi, et al. Optical frequency dissemination via 103-km urban fiber link with remote passive phase stabilization[J]. Optics Express, 2024, 32(13): 23784.

[13] GROSCHE G, TERRA O, PREDEHL K, et al. Optical frequency transfer via 146 km fiber link with 10^{-19} relative accuracy[J]. Optics Letters, 2009, 34(15): 2270-2272.

[14] TERRA O, GROSCHE G, SCHNATZ H, et al. Brillouin amplification in phase coherent transfer of optical frequencies over 480 km fiber[J]. Optics Express, 2010, 18(15): 16102.

[15] MATEI D G, LEGERO T, HÄFNER S, et al. 1.5 μm lasers with sub-10 mHz linewidth[J]. Physical Review Letters, 2017, 118(26): 263202.

[16] HÄFNER S, FALKE S, GREBING C, et al. 8×10^{-17} fractional laser frequency instability with a long room-temperature cavity[J]. Optics Letters, 2015, 40(9): 2112-2115.
[17] CAMPBELL L S, HUTSON R, MARTI G, et al. A Fermi-degenerate three-dimensional optical lattice clock[J]. Science, 2017, 358(6359): 90-94.
[18] YANG Y A, MIKLOS M, TSO Y, et al. Clock precision beyond the standard quantum limit at 10^{-18} level[J]. Physical Review Letters, 2025, 135(19): 193202.
[19] WILLIAMS A, SWANN W C, NEWBURY N R. High-stability transfer of an optical frequency over long fiber-optic links[J]. Journal of the Optical Society of America B, 2008, 25(8): 1284-1293.
[20] NEWBURY N R, WILLIAMS P A, SWANN W C. Coherent transfer of an optical carrier over 251 km[J]. Optics Letters, 2007, 32(21): 3056-3058.
[21] LOPEZ O, HABOUCHA A, KÉFÉLIAN F, et al. Cascaded multiplexed optical link on a telecommunication network for frequency dissemination[J]. Optics Express, 2010, 18(16): 16849.
[22] HU Liang, TIAN Xueyang, WU Guiling, et al. Passive optical phase noise cancellation[J]. Optics Letters, 2020, 45(15): 4308-4311.
[23] ZHANG Xiang, HU Liang, DENG Xue, et al. Passively stable dissemination of ultrastable optical frequency via a noisy field fiber network[J]. Optics & Laser Technology, 2023, 157: 108738.
[24] TERRA O. Dissemination of ultra-stable optical frequencies over commercial fiber networks[D]. PhD thesis, 2010.
[25] PREDEHL K. A 920 km optical fiber link for frequency metrology at the 19th decimal place[D]. PhD thesis, 2012.
[26] DENG Xue, LIU Jie, ZANG qi, et al. Coherent phase transfer via fiber using heterodyne optical phase locking as optical amplification[J]. Applied Optics, 2018, 57(32): 9620-9624.
[27] XU Dan, LEE W K, STEFANI F, et al. Studying the fundamental limit of optical fiber links to the 10^{-21} level[J]. Optics Express, 2018, 26(8): 9515-9527.
[28] ZANG Qi, QUAN Honglei, ZHAO Kan, et al. High-precision time-frequency signal simultaneous transfer system via a WDM-based fiber link[J]. Photonics, 2021, 8(8): 12.
[29] CHEN Ding, XU Jiangning, WU Miao, et al. Optical fiber time synchronization technology based on double fiber round-trip ratio method[J]. Laser & Optoelectronics Progress, 2021, 58(17): 1706001.
陈丁，徐江宁，吴苗，等. 基于双纤环回比值法的光纤时间同步技术[J]. 激光与光电子学进展，2021，58(17)：1706001.
[30] CHEN Faxi, LI Bo, GUO Baolong. Ultra-high precision time transfer based on fiber frequency transfer[J]. Acta Optica Sinica, 2022, 42(15): 1506002.
陈法喜，李博，郭宝龙. 基于光纤频率传递的高精度时间传递方法[J]. 光学学报，2022，59(3)：1506002.
[31] WANG Dan, DENG Xue, LIU Jie, et al. Optic frequency transfer via fiber based on digital phase unwrap technology[C]. 2023, Joint Conference of the European Frequency and Time Forum and IEEE International Frequency Control Symposium (EFTF/IFCS).
[32] SINCLAIR L C, DESCHÊNES J D, SONDERHOUSE L, et al. A compact optically coherent fiber frequency comb[J]. Review of Scientific Instruments, 2015, 86(8): 081301.
[33] CHIODO N, QUINTIN N, STEFANI F, et al. Cascaded optical fiber link using the internet network for remote clocks comparison[J]. Optics Express, 2015, 23(26): 33927-33937.
[34] KREHLIK P, ŚLIWCZYŃSKI Ł, TURZA K, et al. Controlling of the bidirectional amplifier chain for optical frequency distribution based on a two-dimensional noise detector[J]. Optics Express, 2023, 31(8): 12083-12096.
[35] WANG Dan, LIU Jie, JIAO Dongdong, et al. Purification technique with a hertz-linewidth laser for fiber-based optical frequency coherence dissemination[J]. Optical Fiber Technology, 2024, 87: 103923.

Investigation of Phase Noise Compensation Methods for Optical Frequency Transfer

DENG Xue[1,2,3], XUE Wenxiang[1,2,3], HE Zaimin[1,2,3], GUANG Wei[1,2,3], ZHANG Xiang[4], JIAO Dongdong[4]

(1 *School of Communications and Information Engineering, Xi'an University of Posts and Telecommunications, Xi'an* 710121, *China*)

(2 *Shaanxi Key Laboratory of Information Communication Network and Security, Xi'an University of Posts & Telecommunications, Xi'an* 710121, *China*)

(3 *The Youth Innovation Team of Shaanxi Universities*, *Xi'an* 710600, *China*)
(4 *National Time Service Centre*, *Chinese Academy of Sciences*, *Xi'an* 710600, *China*)

Abstract: Phase noise induced by transmission media, such as optical fiber or free-space, is a primary factor influencing the quality of transferred optical signals. Conventional active or passive noise cancellation schemes are fundamentally limited by the intrinsic round-trip propagation delay of their transfer links, resulting in a degradation of phase-locked loop bandwidth and suppression capability as the transmission distance increases. This paper proposes an enhanced compensation method that synergistically combines real-time cancellation with post-processing. By temporally aligning the compensation signal with the noise signal before cancellation, the impact of fiber delay is reduced, thereby improving noise suppression performance. The proposed enhanced phase noise compensation method is applicable to both active and passive noise cancellation schemes. It utilizes an additional measurement of the free-running beat signal alongside the real-time compensation signal. By taking the difference between the phase of the free-running beat signal and that of the real-time compensation signal with a delay of 1.5 τ, a correction signal is generated. At the user end, the transmitted signal is delayed by 0.5 τ and differentially processed with the correction signal to achieve enhanced phase noise suppression. In the passive compensation scheme, the free-running signal itself serves as the compensation signal, which is delayed by 1.5 τ. Theoretical analysis reveals that the noise suppression capability of the proposed method is 4 times that of the conventional active scheme and 28 times that of the passive scheme. To validate the method, a 300 km fiber - based optic frequency transfer simulation was conducted. The fiber was divided into 30 segments to model phase noise accumulation during laser transmission, and a phase noise model based on the power spectral density characteristics of actual fiber links was adopted. The simulation was performed with a sampling rate of 20 kHz and 10^7 sampling points. The results demonstrate that the proposed enhanced method significantly outperforms conventional active and passive compensation techniques. The simulation results show that the Modified Allan Deviation (MDEV) at an averaging time of 1 second is 2.8×10^{-13} for the free-running link, 1.6×10^{-15} for the passive method, 8.0×10^{-16} for the active method, and 3.3×10^{-16} for the enhanced method, representing an improvement over the active method and a factor of four over the passive method. The method was also verified on a 490 km communication fiber link. The real-time transferred signal and the free-running in-loop signal were simultaneously measured using the same frequency counter. By post-adjusting their relative delay according to the proposed method and taking their difference, enhanced phase noise suppression was achieved. The relative delay was adjusted using the counting measurement interval of 1 ms, with the nearest achievable delay being 1.41 τ. The instability of the proposed enhanced suppression scheme is significantly improved compared to the conventional passive locking method, with an ADEV improvement factor of approximately 4.37 at 1 second, thereby validating the effectiveness of the scheme. The study also investigated the impact of time synchronization deviations between the two ends of the link on compensation performance and simulated the suppression of cycle slips caused by the limited dynamic range of the phase detector in the active scheme. Regarding time synchronization accuracy, optimal enhancement is achieved when $\delta\tau = 1.5\ \tau$. Deviations within $\pm 0.1\ \tau$ maintain 90% of the optimal performance, corresponding to approximately 0.15 milliseconds for a 300 km fiber link—a technically achievable requirement. Furthermore, the proposed method effectively eliminates cycle slips induced by the limited dynamic range of the phase detector through post-processing, thereby further improving transfer accuracy. In summary, this paper proposes an enhanced phase noise compensation method for optical frequency transfer links. By performing real-time compensation of the transmitted signal at the local end, measuring the phase noise compensation correction signal, and subsequently removing the correction signal from the transmitted signal via post-processing, the method significantly improves link performance. Simulations and practical experiments validate the theoretical derivations. The results show that the transfer instability of the proposed method is four times better than that of conventional passive schemes. The study also analyzes the impact of time synchronization errors on system performance and verifies the suppression of cycle slips. This method is applicable to high-precision optical frequency transfer systems and provides a valuable reference for research and development in related fields.

Key words: Fiber optics links and subsystem; Phase noise cancellation; Frequency transfer; Fiber; free space

OCIS Codes：060.2360；120.3940；140.3425
CSTR：32255.14.gzxb20265508.0806002

Foundation item：National Natural Science Foundation of China（12403078，12303077），Xi′an Association for Science and Technology Young Talent Support Program Project（0959202513075），the Key Research and Development Program of Shaanxi Province（2024GX-ZDCYL-01-28，2025CY-YBXM-0060），the Sanqin Talents′ Special Support Program（09R0557A00），the Shaanxi Provincial Outstanding Young Scientist Fund Project（2025JC-JCQN-082），the Shaanxi Province Qin Chuangyuan "Scientist ＋ Engineer" Team Construction Project（2025QCY-KXJ-162）